

Bond Strength and Performance of Optical Fibre Bragg Gratings Sensors Embedded in Composite Patch Repairs for Military Aircraft

Tyler P. JONES¹, Tom THORVALDSEN¹, Geir SAGVOLDEN², Karianne PRAN² and Torbjørn OLSEN¹

¹ Norwegian Defence Research Establishment (FFI). Instituttveien 20, NO-2027 Kjeller, NORWAY
tyler.jones@ffi.no, tom.thorvaldsen@ffi.no, torbjorn.olsen@ffi.no
² Light Structures AS, Nils Hansens vei 2, NO-0667 Oslo, NORWAY
geir.sagvolden@lightstructures.no, karianne.pran@lightstructures.no

Abstract

Structural health monitoring (SHM) systems are recognized as a key element in a modern and efficient approach to structural lifecycle management. With novel applications of advanced materials, such as extensive use of fibre reinforced composites on aircraft, further advances in monitoring and inspection techniques are required. This is especially relevant for repairs on primary (i.e. load bearing) military aircraft composite structures, where traditional non-destructive inspection methods alone may be insufficient for certification of the repair. Optical fibre sensor systems with continuous in-flight monitoring are considered a promising approach to providing the necessary information on the status of the repaired area.

Fibre optic sensor systems commonly involve the use fibre Bragg grating (FBG) sensors bonded to or embedded in the structure. As an element in a certified repair strategy, the limitations of the load transfer from the structure to the sensor must be known. Hence, extensive analysis and testing must be done before introducing any adhesive system/optical fibre combination as part of the SHM system.

This paper presents experimental test results obtained for the interface properties of optical fibres with polyimide or Ormocer® coating embedded in an adhesive. Three different adhesives, which are all relevant for military aircraft primary composite structural repairs, are included in the test program. A modified fibre pull-out test set-up is applied for estimating the interfacial shear strength (IFSS) for each of the six combinations of adhesive and optical fibre, at two different nominal embedded lengths of 0.5 mm and 1.0 mm. For the polyimide coated fibre, the IFSS values obtained for the three adhesives from fibre pull-out do not differ significantly. The highest IFSS values are obtained at a nominal embedded length of 0.5 mm. The optical fibre with Ormocer® coating seems to have the strongest bond to the adhesives, but results in core pull-out instead of fibre pull-out. The obtained IFSS values for the core/coating interface of the Ormocer® coated fibre are not directly comparable with the IFSS values obtained for the polyimide coated fibre, but they still demonstrate the load transfer properties and the potential of the optical fibre for obtaining accurate strain measurements. As an overall conclusion, the polyimide coated fibre is considered the most appropriate for use in a fibre optic sensor system for SHM.

Keywords: embedded sensor, adhesive joint, composite, condition monitoring, optical fibre sensor, fibre Bragg grating.



1. INTRODUCTION

For the armed forces in different countries, there is a large focus on reducing the maintenance cost and increase the operational ability. To meet these requirements a new way of thinking, when it comes to maintenance, is needed. For military platforms there is currently a paradigm shift from more traditional periodic maintenance systems to condition-based maintenance systems. That is, instead of inspecting the structure on a periodic basis, for example every week or after each flight or mission, critical parameters are monitored continuously, assuring optimal conditions for the structure.

With the application of new and modern materials, such as fibre composites, other monitoring and inspection techniques are required, compared to those applied for more traditional materials, such as metals. Moreover, with novel applications of advanced materials, the maintenance personnel may not have the same hands-on, long-term experience with the behaviour of the materials. Establishing new systems for monitoring are especially relevant for the health monitoring of “drop-outs”, which are unexpected damage situations, such as repairs of primary (i.e. load bearing) composite structures. For certification of such repairs, the more traditional non-destructive inspection methods may be insufficient, according to international flight regulations authorities (e.g. FAA and EASA), and hence alternative methods must be established and applied. Structural health monitoring (SHM) systems may thus be the solution to these new challenges, as part of a modern condition-based maintenance concept.

Fibre optics systems have been demonstrated and applied for monitoring of military aircraft and naval ships [1]. Even though the level of maturity for SHM system is relatively high, there is, in general, still a gap between the available technology and the requirements set by the operators in each case. The use and integration of SHM systems monitoring a *bolt free* repair of the primary composite structure of a military helicopter, is one such example.

Different technologies may be considered for an SHM system on a military platform, such as strain gauges, piezoelectric actuators or more traditional non-destructive methods. However, fibre optics sensor systems with continuous data logging possibilities during operation seem to be one of the most promising approaches for efficient monitoring of modern structures. In particular, optical fibre sensors have small size and low weight, they have a non-electrical nature (i.e. immune to electromagnetic interference and electrical noise), do not degrade over time (as traditional strain gauges), have a capability to be multiplexed in a single optical fibre (to reduce the number and weight of cables), have material integretability, and can withstand high dynamic loads [1;2]. Optical fibres with fibre Bragg gratings (FBGs) have been commonly used, see e.g. [3-6], but other measuring techniques may also be applicable, such as backscattering techniques [1;7].

In case of using optical fibre sensors, they could be inserted between the plies of a patch (in a wet lay-up repair procedure), at the bondline between a pre-cured patch and the structure, or at the surface of the structure/repair. For any location and case, the use of optical fibre monitoring systems requires that the optical fibre sensors give accurate and precise strain measurements due to the applied loads (mechanical or thermal). The load transfer from the structure to the optical fibre is one essential part of the system that needs to be considered. In particular, one must make sure that the adhesive will not degrade the optical fibre or the

composite structure over time, due to environmental factors, such as temperature variation, diffusion of water, salt, and contamination, such as oil and fuel. Hence, extensive analysis and testing must be done before introducing any adhesive/optical fibre combination as part of the optical fibre SHM system.

In this paper, experimental results from a test program on the load transfer properties between optical fibres and adhesive systems are presented. Two different optical fibres are considered; a polyimide coated fibre and a fibre with Ormocer® coating. Three different adhesives, which are all relevant for repair of military helicopters, are included. For each of the six combinations of optical fibre and adhesive, a modified fibre pull-out set-up is established for estimating the interfacial shear strength (IFSS). The IFSS value is an indicator of the load transfer capacity between the adhesive and the fibre, and may be employed when considering the durability and robustness of different adhesive/optical fibre combinations.

2. MATERIALS AND OPTICAL FIBRES

In this test program, two different optical fibres are included. The first optical fibre has a PYROCOAT® polyimide coating, and is produced by OFS and delivered by Technica. This optical fibre has a core of glass with a diameter of 125 μm . The total diameter of the fibre (including the polyimide coating) is 150 μm . For this fibre, the original coating is removed when inscribing the FBGs. After the sensor inscription, the FBG sensor area is recoated. Different load transfer and bonding properties may be experienced due to this. The second optical fibre has an Ormocer® coating, and is produced and delivered by FBGS International. This optical fibre is made using the draw tower procedure, and the FBGs are inscribed in the fibre before applying the coating, and, hence, no re-coating is needed. This is considered as more gentle to the glass core, compared to the re-coating process, avoiding micro-cracks and defects, which again can influence on the maximal strain tolerance. The FBGS International fibre has a core of glass with a diameter of 125 μm , whereas the total diameter of the fibre (including the coating) is 190 μm . It should be noted that the fibres employed in the testing do not include the FBG sensor area of the fibres due to the number of test samples and the relatively high cost of each optical fibre with FBGs.

Due to strict requirements and certification of all materials applied for aircraft/helicopters, there is reduced flexibility for the choice of adhesive. Three different adhesives, which are applicable to military aircraft, are considered: Loctite EA 9394 QT AERO (same as Hysol EA 9394) [8], Loctite EA 9395 QT AERO [8], and Epocast 52 [9]. The Epocast 52 system has a very low viscosity, and is typically used as a resin in fibre composites, among others for wet lay-up. The Loctite systems have a much higher viscosity, and are typically applied as pastes for bonding of pre-cured composite components and pre-cured patch repairs of composite structures.

To the authors' knowledge no IFSS data are available in the open literature for the pull-out load transfer properties of the combinations of optical fibres and adhesives considered in this test program. Direct comparison with other data is therefore not possible.

3. EXPERIMENTAL TESTING

3.1 Test method and sample preparation

Different test methods have been established for estimating the bonding and shear properties between fibres and the surrounding matrix/adhesive, see e.g. [10-12], where the embedded single-fibre tension test and the microbond test are most commonly used [13]. These tests are applied both for reinforcing fibres, as well as for optical fibres. In the single-fibre tension test, one single fibre is embedded in a dog bone shaped test specimen, a crack is introduced, and the fibre is pulled out in tension. For the microbond test set-up, a small droplet of adhesive is applied to a single fibre, and the cured adhesive is pulled off the fibre in tension. The interfacial shear strength (IFSS) is estimated according to the following expression:

$$\tau_{IFSS} = \frac{P}{\pi dl} \quad (1)$$

where P is the applied tensile load, and the denominator expresses the surface area of the fibre surrounded by adhesive, with d being the fibre diameter and l the embedded fibre length.

Several challenges have been reported for the microbond test, among others due to the varying shape of the adhesive droplet and the positioning of the knives included in the test set-up for pulling off the adhesive, see e.g. [11;14]. To improve the repeatability of the test, Morlin and Czigany [14] introduced a cylindrical shaped adhesive to avoid the droplet shape variation, and to simplify the pull-out of the fibres from the adhesive by instead applying the force on the metal plate surrounding the adhesive. To get test samples where the fibre is centred in the adhesive cylinder, and where the fibre is perpendicular to the surface of the adhesive surface, a special rig was made. This set-up also requires that the bottom is cut off and polished before testing, which may introduce micro-cracks or other defects in the specimen at or close to this surface.

In the current test program, a new variant of the Morlin and Czigany microbond test is suggested, which in this paper will be referred to as a fibre pull-out test. In our modified test set-up, each test specimen consists of a polycarbonate tab, with a 1.5 mm diameter cylindrical flat bottomed hole machined at a depth h , as shown in Figure 1. This hole diameter makes it possible to fill the hole with adhesive using a syringe. The hole depth is either 0.5 mm or 1 mm. Initial fibre-only ultimate tensile failure tests (using a Zwick BZ2.5/TN1S material testing machine) have been performed to determine the failure strengths and tensile behaviour for the two types of optical fibres, and hence suitable embedded lengths to ensure that adhesive-fibre debonding occurs before non-linear behaviour is introduced in the fibre, or the fibre itself fails. The optical fibre is embedded at the centre of the hole at a nominal depth equal to the hole depth, before curing according to the manufacturer's curing cycle. The specimens with Epocast 52 were cured at 66°C for 3 hours. The Loctite specimens (both types) were cured at 66°C for 1 hour. After curing, paper tabs were bonded to the free fibre ends using cyanoacrylate adhesive, to provide a suitable gripping area that would not damage the embedded optical fibres.

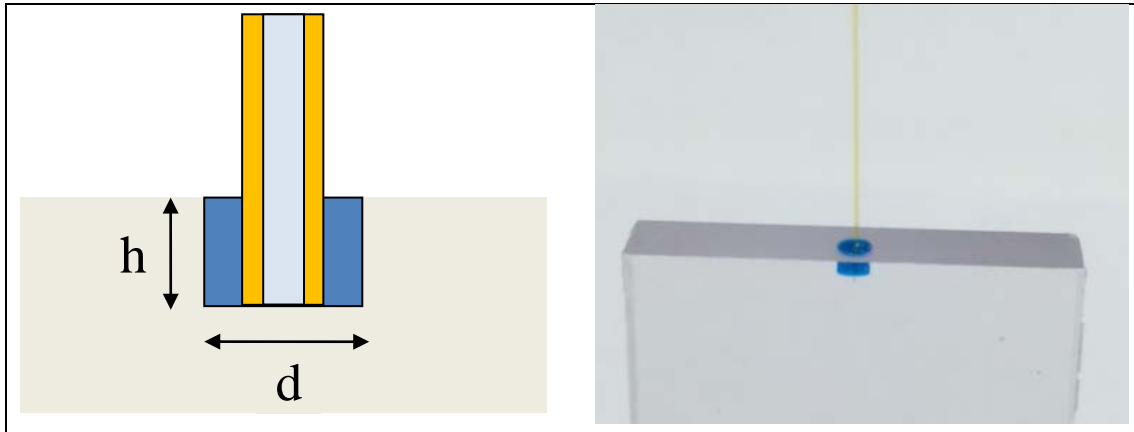


Figure 1: Left: Sketch of the fibre (core and coating) embedded in the adhesive, which is filled in the hole made in the polycarbonate tab. The size of the hole is given by the height h and the diameter d , and the nominal embedded length is equal to the hole height. Right: The produced test specimen.

3.3 Test program

Twelve different sets of test specimens were made; six different combinations of adhesive and optical fibre, and two different embedded lengths. For each set, 8-10 specimens were prepared and tested and included in the IFSS calculations. Each test specimen was given a unique test ID, IFSS-X-Y, where the X denotes the specimen set number, and Y denotes the specimen number in each set. The test specimen ID is used as reference in the following, and more details for each set are found in Table 1 and Table 2.

The pull-out testing in tensile mode was performed on the same material testing machine as the fibre-only tests, controlled by the testXpert II software package. The specimens were loaded vertically in the tensile machine and gripped by the polycarbonate and paper tabs. Displacement control with a crosshead speed of 0.25 mm/min was applied to the specimens, and a load cell recorded load values. Displacement data (for both the free fibre and adhesive/fibre specimens) were recorded with an extensometer that was affixed to grip extensions. Testing was stopped when a reduction of 80% load was observed. The testing was conducted at ambient; approximately 22°C.

Post-test microstructural characterization was accomplished with a Zeiss Stemi 2000-C microscope and images recorded with an Amscope Digital Eyepiece camera. ImageAccess EasyLab software was used to measure the embedded lengths of the fibres using scale based calibrated measurements.

3.4 Test results

The load-displacement curve for test specimen IFSS-1-5 is shown in Figure 2a, i.e. test specimen number 5 in the set using the combination Epocast 52/polyimide coated fibre, and a nominal embedded length of 1 mm. This curve is representative for all the pull-out tests including the polyimide coated fibre. As can be observed, the load increases as a linear function of the displacement. At a certain point, the load drops, resulting in a “kink” on the curve. Thereafter, the load increases as a function of increasing displacement until a peak load, where the test stops (due to the sudden load drop). This peak load is applied in the expression in (1) for calculating the IFSS value for this specimen set.

Cured Epocast 52 is transparent, and allows for inspection of the adhesive/fibre interface after testing. From the microstructural characterization of same test specimen (IFSS-1-5), see Figure 3, one can observe conical cracks both close to the fibre end and close to the surface of the embedded fibre. Similar behaviour is observed for all the test specimen sets including the polyimide coated fibres (both embedded lengths) in the test program.

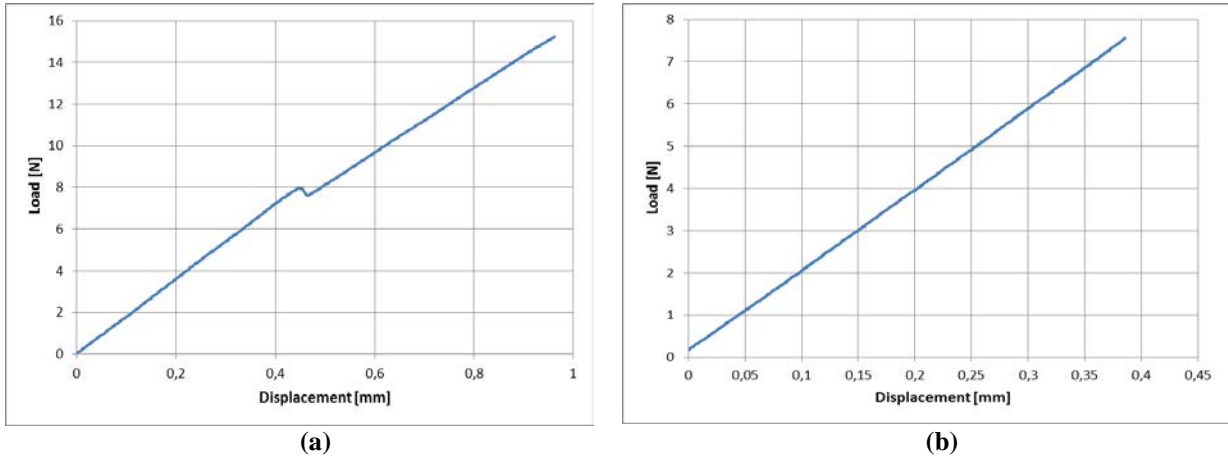


Figure 2: Load-displacement curves for a) IFSS-1-5 and b) IFSS-6-6.

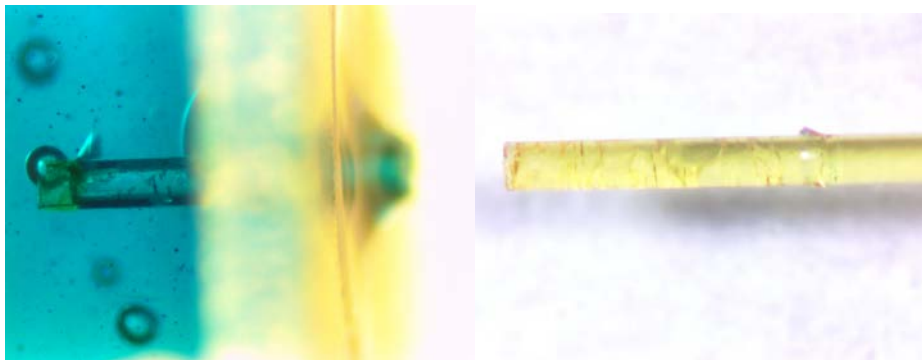


Figure 3: Micrograph of test specimen IFSS-1-5. Left: Example of conical crack formation in the Epocast 52 adhesive. Right: Fibre after pull-out; cracks are observed in the coating.

For the tested specimen sets including the Ormocer® coated fibres, failure along the glass fibre core led to a pull-out of the glass core from the coating. Reducing the embedded length from 1 mm to 0.5 mm did not alter this behaviour. The micrograph after glass core pull-out is shown in Figure 4 for specimen IFSS-6-6, i.e. specimen 6 for the combination Loctite EA 9395 QT AERO/Ormocer® coated fibre, and an embedded length of 1 mm. The glass core can be clearly seen to have separated from the protective coating of the optical fibre. Further investigation of the non-embedded fibre length also showed regions of glass/coating delamination.

Since the fibre fails at the glass core/coating interface, the adhesive/fibre IFSS value cannot be determined in the same way as for the polyimide coated fibre cases. The load-displacement curve for IFSS-6-6 is shown in Figure 2b. In this case, no “kink” is observed, and the core seems to be pulled out without any crack propagation. This curve is representative for the pull-out tests of the specimen set including the Ormocer® coated fibre.

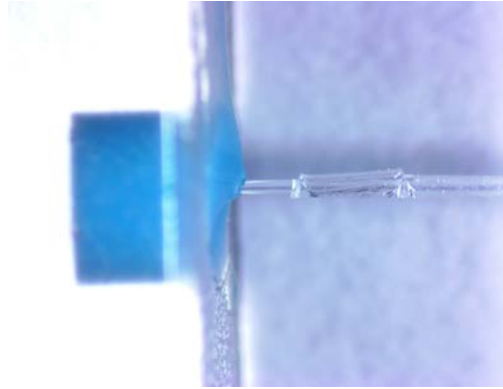


Figure 4: Micrograph of test specimen IFSS-6-6. Glass core pull-out.

Table 1 and Table 2 summarize the failure load and the estimated IFSS for the twelve different sets of specimens included in this test program. The total fibre diameter (including the coating) is applied in the calculation of the IFSS value for the test specimens including the polyimide coated optical fibre (Table 1), whereas for the test specimens including the Ormocer® coated optical fibre (Table 2) the glass core diameter is applied. From Table 1, we observed that there are only small variations in the IFSS values for the three adhesives. The highest mean IFSS values were obtained at a nominal embedded length of 0.5 mm. Moreover, the average failure load for the nominal embedded length of 1 mm was found to be around twice the failure load for the nominal embedded length of 0.5 mm. The IFSS values obtained for the combinations including the Ormocer® coated optical fibres do not vary significantly, but are slightly higher for the nominal embedded length of 0.5 mm, see Table 2. In this latter case, the average failure load is almost constant and independent of nominal embedded length.

Test ID	Adhesive system	Optical fibre coating	Average failure load (N)	Average embedded length (µm)	IFSS (MPa)
IFSS-1	Epocast 52	Polyimide	20	944	46 ± 10
IFSS-2	Loctite EA 9394 QT AERO	Polyimide	19	732	53 ± 7
IFSS-3	Loctite EA 9395 QT AERO	Polyimide	23	969	52 ± 6
IFSS-7	Epocast 52	Polyimide	9	330	69 ± 9
IFSS-8	Loctite EA 9394 QT AERO	Polyimide	10	370	61 ± 10
IFSS-9	Loctite EA 9395 QT AERO	Polyimide	13	485	58 ± 6

Table 1: Average failure load, average embedded length and estimated interfacial shear strength (IFSS) values for the adhesive/polyimide coated fibre combinations.

Test ID	Adhesive system	Optical fibre coating	Average failure load (N)	Average embedded length (in μm)	IFSS (in MPa)
IFSS-4	Epocast 52	Ormocer	11	610	49 ± 9
IFSS-5	Loctite EA 9394 QT AERO	Ormocer	10	583	44 ± 7
IFSS-6	Loctite EA 9395 QT AERO	Ormocer	11	674	44 ± 11
IFSS-10	Epocast 52	Ormocer	9	395	60 ± 13
IFSS-11	Loctite EA 9394 QT AERO	Ormocer	8	379	55 ± 11
IFSS-12	Loctite EA 9395 QT AERO	Ormocer	8	453	47 ± 10

Table 2: Average failure load, average embedded length and estimated interfacial shear strength (IFSS) values for the adhesive system/Ormocer® coated fibre combinations. The IFSS at the core/coating interface is calculated in this case.

4. DISCUSSION

According to the mathematical model established by Hampe *et al.* [15], the simulated load-displacement trace for the fibre/adhesive system can be divided into four different stages, or parts, during fibre pull-out. In the first stage, the load is increased by loading the free fibre end. The interface is still intact, and the system follows Hooke’s law of elastic deformation. The shear stress at the interface increases with the displacement, with the highest stress concentrations at the matrix surface (not at the fibre end). In the next stage, the crack grows along the fibre surface. The crack length and the stresses at the fibre end increases as the displacement increases. In the third stage, the propagation of the crack is accelerated, and only small displacements results in higher crack propagation speeds than for the previous stage. A peak pull-out load is reached before entering the final stage, where the entire fibre is debonded and pulled out. The load required to pull out the fibre is much lower than the peak load, and is due to friction at the interface. Such behaviour is observed for the test specimens with the polyimide coated fibres, where a “kink” is observed. This is probably due to the initiation of interface cracks and matrix cracks. The fourth stage is not seen in Figure 2a, due to the sudden load drop at pull-out that stops the test. Similar interface and matrix crack formations as shown in Figure 3 have been described by Pegoretti *et al.* [16] for single-fibre pull-out of glass fibres with different sizings and/or coupling agents. The elastic polyimide coating may give different orientations of the cracks (i.e. the angle the conical cracks make with the interface) compared to a structural fibre without coating. The same pull-out crack formation behaviour has, however, not been observed for the Ormocer® fibres. Instead of fibre pull-out, core pull-out was observed. Reducing the embedded length from 1 mm to 0.5 mm did not change this behaviour. This indicated that the bonding between the adhesive and the coating is higher than the bonding between the coating and the glass core. Furthermore, the linear load-displacement curve in Figure 2b indicates that no crack has propagated along any of the two interfaces (core/coating and coating/adhesive), and that there is just a sudden core release/pull-out at a certain (peak) load.

With the obtained results, no one-to-one comparison between the two types of optical fibre

can be done, since the test set-up gave a different behaviour for the two fibres. For the fibre “system” as such (i.e. core and coating), the shear strength has generally been found to be higher for the polyimide fibres. On the other side, the bonding between the fibre coating and adhesive is probably better for the Ormocer® fibre, and, in particular there is a higher shear load capacity at the adhesive/coating interface compared to the core/coating interface. Despite the improved bonding properties, it is the load transfer from the adhesive to the optical fibre which is the most important. If the core is moving relative to the coating, the deformation of the adhesive/structure cannot be measured. Overall, the polyimide coated fibre is therefore considered the best choice. For comparison, Schukar *et al.* [2] tested the same two types of optical fibres, and concluded from their fibre push-out test program that the Ormocer® coated fibre has a higher IFSS between the fibre and the adhesive compared to the polyimide coated fibre. They still (also) ranked the polyimide coated fibre higher than the Ormocer® fibre due to the applicability for accurate strain measurements.

A simple analytical expression is applied for the relatively complex pull-out process, with shear variations along the embedded fibre length [17]. The applied expression for the IFSS is only an average value, and the expression is only valid in case the stress field is homogeneous, which can be obtained in case the fibre load is high enough, so that the complete adhesive zone along the fibre is yielded, or in case there is a complete debonded fibre with a friction stress equal to the interface shear stress [15]. Moreover, as the embedded length is shortened, the average IFSS value calculated in (1) will approach the shear strength value for the interface. More detailed models for the load transfer, taking into account the shear stress variation along the fibre, as well as the properties of both the core coating and adhesive, see e.g. [18], may be required to get a more precise estimate of the bonding properties. This is beyond the aim of this paper.

5. SUMMARY AND CONCLUSIONS

In this paper, a modified fibre pull-out test set-up has been applied for estimating the bonding properties between optical fibres and adhesives that are relevant for primary aircraft structure repairs. Two different optical fibres and three adhesives are included in the test program. The load transfer from the adhesive to the optical fibre is very important for the fibre to be applied as a sensor in a structural health monitoring sensor system, where accurate measurements of axial strains are essential.

The two fibres gave different load transfer properties for the same three adhesives. For the sets of test specimens with a combination of adhesive and polyimide coated fibres, the average IFSS value for the three adhesives ranged from 46 to 53 MPa for the 1 mm nominal embedded length, and from 58 to 69 MPa for the 0.5 mm nominal embedded length. The bonding properties of the three adhesives were thus quite similar. Moreover, the average failure load for the longest nominal embedded length was found to be around twice the failure load for the shortest embedded length, indicating that the crack propagation is a function of the embedded length. The IFSS values for the 0.5 mm nominal embedded length are believed to be closest to the real value experienced along the fibre length during pull-out, since the calculated IFSS is an average value that approaches the “real” value as the embedded length is reduced. For the sets of test specimens with a combination of adhesive

and Ormocer® coated fibres, a core pull-out was obtained – irrespective of embedded length. The calculated average IFSS value (in this case using the core diameter in the IFSS expression) for the three adhesives ranged in this case from 44 to 49 MPa for the 1 mm nominal embedded length, and from 47 to 60 MPa for the 0.5 mm nominal embedded length. In this case, the average failure load was almost the same and independent of nominal embedded length, indicating no crack propagation and just an ultimate pull-out load.

The results are not directly comparable, as different pull-out characteristics are observed. The Ormocer® coated fibre has probably a stronger bond to the adhesive compared to the polyimide fibre. However, there is a better control of the load transfer from the adhesive to the fibre for the polyimide coated fibre. The polyimide coated fibre is therefore considered the best alternative for accurate strain measurements.

Future work will consider more advanced mathematical models for estimating the “real” interfacial shear properties, and to get a better understanding of the bonding characteristics during the different stages of the fibre pull-out. As the polyimide coated fibre is recoated in the FBG sensor area, performing pull-out tests with the FBG sensors embedded in the adhesive is a relevant next step. Moreover, a study of the properties and behaviour of the adhesive/optical fibre properties in different conditions, such as temperature variations combined with varying humidity, as well as the influence from contamination, will also be relevant.

ACKNOWLEDGEMENTS

This work has been conducted as part of Project B-1324-GEM1-GP (PATCHBOND) of the European Defence Agency, funded by The Netherlands, Germany, Spain, Finland and Norway. The authors would like to give a special thanks to Dr. Ing. Malte Frövel (INTA, Spain) for providing the Ormocer® fibre.

REFERENCES

- [1] "Structural health monitoring of military vehicles," NATO Science&Technology Organization (STO), STO-EN-AVT-220, 2014.
- [2] V. Schukar, N. Kusche, G. Kalinka, and W. Habel, "Field deployable fiber Bragg grating strain patch for long-term stable health monitoring applications," *Applied Sciences*, **3**, 39-54, 2013.
- [3] L. F. M. da Silva, P. M. G. P. Moreira, and A. L. D. Loureiro, "Determination of the strain distribution in adhesive joints using fiber Bragg grating (FBG)," *Journal of Adhesion Science and Technology*, **28**, 1480-1499, 2014.
- [4] K. I. Tserpes, V. Karachalios, I. Giannopoulos, V. Prentzias, and R. Ruzek, "Strain and damage monitoring in CFRP fuselage panels using fiber Bragg grating sensors. Part I: Design, manufacturing and impact testing," *Composite Structures*, **107**, 726-736, 2014.
- [5] R. Ruzek, P. Kudrna, M. Kadlec, V. Karachalios, and K. I. Tserpes, "Strain and damage monitoring in CFRP fuselage panels using fiber Bragg grating sensors. Part II:

- mechanical testing and validation," *Composite Structures*, **107**, 737-744, 2014.
- [6] L. P. Canal, R. Sarfaraz, G. Violakis, J. Botsis, V. Michaud, and H. G. Limberger, "Monitoring strain gradients in adhesive composite joints by embedded fiber Bragg grating sensors," *Composite Structures*, **112**, 241-247, 2014.
- [7] J. H. L. Grave, M. L. Håheim, and A. T. Echtermeyer, "Measuring changing strain fields in composites with distributed fiber-optic sensing using the optical backscattering reflectometer," *Composites Part B*, **74**, 138-146, 2015.
- [8] "Henkel adhesives; www.henkel-adhesives.com," 2016.
- [9] "Huntsman Advanced Materials, www.huntsman.com," 2016.
- [10] M. J. Pitkethly, J. P. Favre, U. Gaur, J. Jakubowski, S. F. Mudrich, D. L. Caldwell, L. T. Drzal, M. Nardin, H. D. Wagner, L. Di Landro, A. Hampe, J. P. Armistead, M. Desaegeer, and I. Verpoest, "A round-robin programme on interfacial test methods," *Composites Science and Technology*, **48**, 205-214, 1993.
- [11] S. Sockalingam and G. Nilakantan, "Fiber-matrix interface characterization through the microbond test," *International Journal of Aeronautical and Space Sciences*, **13**, 282-295, 2012.
- [12] A. Fjeldly, T. Olsen, J. H. Rysjedal, and J. E. Berg, "Influence of the fiber surface treatment and hot-wet environment on the mechanical behavior of carbon/epoxy composites," *Composites Part A*, **32**, 373-378, 2001.
- [13] D. Adams, "Fiber-matrix interfacial bond test methods," 2011.
- [14] B. Morlin and T. Czigany, "Cylinder test: development of a new microbond method," *Polymer Testing*, **31**, 164-170, 2012.
- [15] A. Hampe, G. Kalinka, S. Meretz, and E. Schultz, "An advanced equipment for single-fibre pull-out test designed to monitor the fracture process," *Composites*, **26**, 40-46, 1995.
- [16] A. Pegoretti, M. L. Accorsi, and A. T. Dibenedetto, "Fracture toughness of the fibre-matrix interface in glass-epoxy composites," *Journal of Materials Science*, **31**, 6145-6153, 1996.
- [17] E. Pisanova, S. Zhandarov, E. Mäder, I. Ahmad, and R. J. Young, "Three techniques of interfacial bond strength estimation from direct observation of crack initiation and propagation in polymer-fibre systems," *Composites Part A*, **32**, 435-443, 2001.
- [18] Z. Zhou, J. Li, and J. Ou, "Interface transferring mechanism and error modification of embedded FBG strain sensors," *Frontiers of Electrical and Electronic Engineering in China*, **2**, 92-98, 2007.